

## A Study on Statistical Probability of Man-Made Impulsive Noises such as Electrostatic Discharge in Urban Environments

Hiroshi HIGUCHI,\* Kenji YAMAUCHI,\* Muneo MAEDA\*  
and Nobuo TAKAHASHI\*

(Received September 26, 1989)

Recently, digital communication or digital communication controls has been made possible by the development of computer technology. However, the effect of most man-made impulsive noise, such as electrostatic discharge caused by machines or human bodies, is observed in communication links. This is not fully understood due to highly non-Gaussian random processes. Middleton proposed the universal statical physical models of impulsive noise for the radio noise, this paper is based on Middleton's exceedance probability models, and is concerned with methods for calculating the bit error rates caused by man-made impulsive noise in communication links located in manufacturing or office area. The results can be applied to find the error rates for many types of the communication links. It is shown the error rate on the communication links is affected by the impulsive noise that is usually encountered in practice.

### 1. Introduction

The principal man-made impulsive noise and natural electromagnetic interference (EMI) models are the so-called Class A, Class B, and Class C types respectively. They are distinguished by input spectral bandwidths (such as narrow-band or broad-band) for electronic receiving circuits. Also three Classes of A, B, and C interference impulsive noise are identified theoretically by Middleton. Henceforth, in this paper, the phrase "interference impulsive noise" is simply written as the "interference."

**Class A interference:** This noise is typically narrow spectrum than the electronic receiving circuits, and generates ignorable transients at the inputs of said circuits when a source emission terminates.

**Class B interference:** The bandwidth of the incoming noise is large than that of the inputs stages of the electronic receiving circuits, so that

transient effects, both in build-up and decay, occur with the latter predominating.

**Class C interference:** This is the sum of the Class A and the Class B interference components.<sup>1)</sup>

The above three interference models are based on a Poisson distribution of sources in space and times, since most man-made impulsive noise such as electrostatic discharge caused by human bodies or machines in a manufacturing or office area.

Figure 1 shows schema of domains ( $x, T$ ) of integration for Class A and B interference. Figure 2 shows an example of an electrostatic discharge transient waveform caused by a human body, Fig. 3 is the propagation of the electrostatic discharge caused by a human body for electronic systems, and Fig. 4 is the impulsive noise waveform of electrostatic discharge induced from the machine. Like this, today's much man-made impulsive noise are produced in urban environments. The purpose of this paper is to experimentally study the Class A interference model and to theoretically apply the Class B interference model on source, such as electrostatic discharge.

**Keywords:** urban environments, electromagnetic inference, impulsive noise, non-Gaussian noise, bit error rate

\* Himeji Institute of Technology, 2167, Shosha, Himeji, Hyogo 671-22, Japan

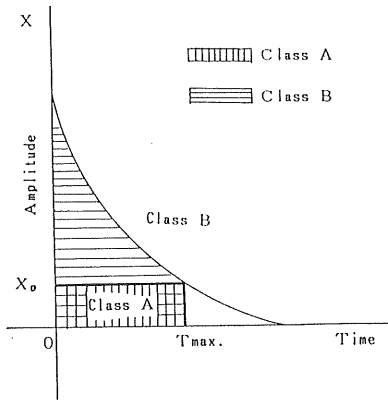


Fig. 1 Schema of domains ( $X, T$ ) of integration for Class A and B interference identified by D. Middleton.<sup>1)</sup>

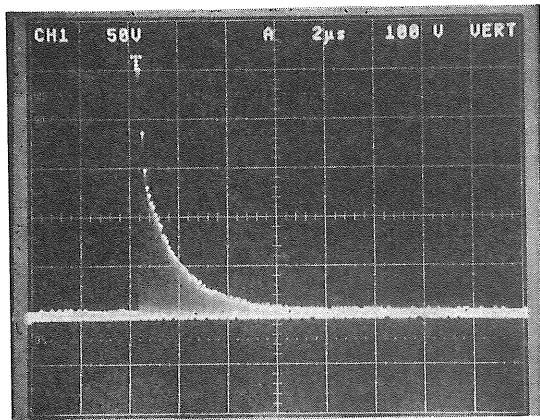


Fig. 2 Electrostatic discharge transient waveform caused by human body.

2. Approach and Experiment

The objective is to determine the narrow-band impulsive noise parameters which fit the measured distribution as defined in Middleton's exceedance probability. Thus, the Class A interference parameters can be estimated from three even-order moments. However, most man-made impulsive noise is of the Class B interference type, such as electrostatic discharge. Therefore, the Class B interference parameters can also apply to the Class A interference model by a similar method, and thus can fit the exceedance probability distribution. These interference impulsive noise are measured on the power line which is connected to measuring equipment by a capacitor coupling. This measuring equipment consist of broad-band type electronic receiving

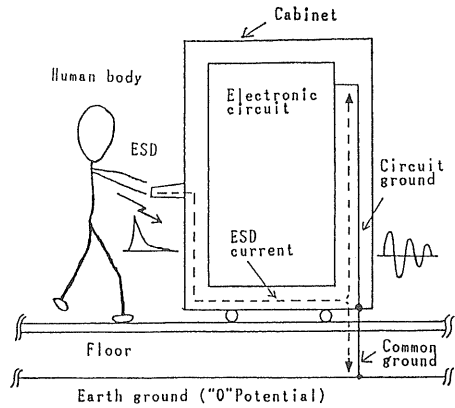


Fig. 3 Propagation of electrostatic discharge by human bodies.

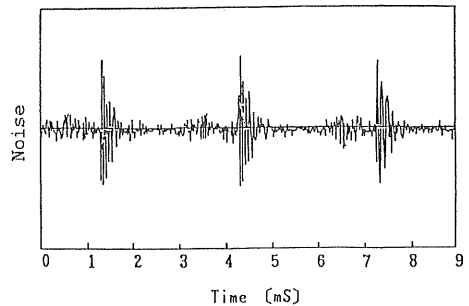


Fig. 4 Impulsive noise induced from machines.

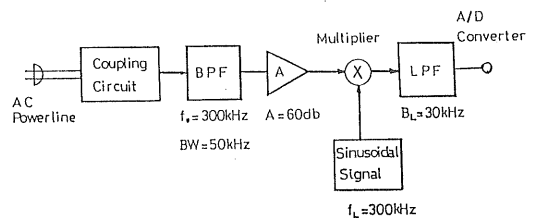


Fig. 5 Block diagram of noise measurement.

circuits. Figure 5 shows the block diagram of noise measurement.

1. Class A Interference Parameters

The Class A interference is described by a three-parameter  $\{A, \Gamma, \Omega_2\}$  model, where  $A$  is "the impulsive index." It is the mean number of emission per second, times the mean duration of a typical interfering source emission,  $\Gamma$  is the "Gaussian factor" or the ratio of the intensity of the independent Gaussian component (of the incoming interference) to the intensity of the impulsive non-Gaussian component, where input interference is concerned.  $\Omega_2$  is the intensity of impulsive component.

The amplitude probability-density function  $P(X)$

for the Class A is written in normalized form.<sup>1)</sup>

$$P(X) \cong \exp(-A) \cdot \sum_{m=0}^{\infty} (A^m/m!) (1/\sqrt{2\pi\sigma_m^2}) \cdot \exp(-X^2/2\sigma_m^2) \quad (1)$$

Where,

$$\sigma_m^2 = \{(m/A) + \Gamma\} / (1 + \Gamma)$$

The amplitude distribution is formed from many Gaussian distribution with different variances  $\sigma_m^2$ .

To determine the parameters for Class A interference, three even-order  $\{X_2, X_4, \text{ and } X_6\}$  moments are desired.<sup>2)</sup>

$$X_{2n} = (1/N) \sum_{i=1}^N X_i^{2n} \quad (2)$$

Where,

$$n = 1, 2, \text{ and } 3$$

These even-order moments of Class A interference are obtained from equation (2), and which gives specifically and exactly.<sup>3)</sup>

$$A = 25(X_4 - 3X_2^2)^3 / 3(X_6 + 30X_2^3 - 15X_2X_4)^2 \quad (3a)$$

$$\Gamma = 3X_2(X_6 + 30X_2^3 - 15X_2X_4) / 5(X_4 - 3X_2^2)^2 - 1 \quad (3b)$$

$$\Omega_2 = 5(X_4 - 3X_2^2)^2 / 3(X_6 + 30X_2^3 - 15X_2X_4) \quad (3c)$$

Above three-parameters are all positive values for Class A interference.

## 2. Class B Interference

The Class B interference model requires the six parameters  $\{A, \Gamma, \Omega_2, A_\alpha, \alpha, Ni\}$ . These parameters are all physically specified and measurable parameters in the analytical model. The first three parameters  $\{A, \Gamma, \Omega_2\}$  are identical to the Class A interference model with the same physical significance as described in Section 2-1. Three additional parameters are required here also.  $A_\alpha$  is an "effective" impulsive index proportional to the impulsive index.  $\alpha$  is the spatial-density propagation parameter which provides an effective measure of the average source density range and  $Ni$  is the scaling factor. The Class B interference model requires two analytical models. One is for the small and intermediate value of the envelope ( $0 < X < X_B$ ), and the other is for the large values ( $X_B < X < \infty$ ); where  $X_B$  is the junction point of these two analytical models as the normalized bend-over point. The principal analytical results here are<sup>4)</sup>:

$$0 < X < X_B$$

$$P(X)_{B-I} \cong \{1/\pi\sqrt{2}(2G_B/N_i)\} \cdot \exp(-\hat{X}^2/2) \cdot \sum_{m=0}^{\infty} \{(-1)^m A^m/m!\} \cdot \Gamma\{(m\alpha+1)/2\} \cdot {}_1F_1(-m\alpha/2, 1/2; X^2/2) \quad (4)$$

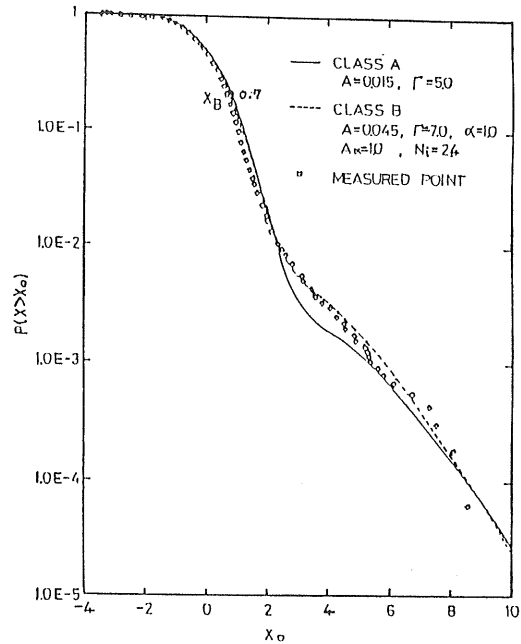


Fig. 6 Schema of exceedance probability for amplitude of the Class A and B interference model.

Where,

$$\hat{A} = X_\alpha / 2^\alpha G_B^\alpha$$

$$\hat{X} = XNi / 2G_B$$

$$G_B^2 = (1/4)(1 + \Gamma)^{-1} \{(4 - \alpha)/(2 - \alpha) + \Gamma\}$$

$\Gamma(\cdot)$ : Gamma function

${}_1F_1(\cdot, \cdot; \cdot)$ : Confluent Hyper-Geometric function

Equation (4) is the Class B interference analytical model which is normally used.<sup>4)</sup>

$$X_B < X < \infty$$

$$P(X)_{B-II} = \exp(-A) \sum_{m=0}^{\infty} (A^m/m!) \cdot (1/\sqrt{2\pi\hat{\sigma}_m^2}) \cdot \exp(-X^2/2\hat{\sigma}_m^2) \cdot (1/4G_B^2) \quad (5)$$

Where,

$$\hat{\sigma}_m^2 = (m/A + \Gamma) / 1 + \Gamma$$

$$\hat{A} = A(2 - \alpha) / 4 - \alpha$$

Equation (5) is modified from equation (1). Here, the  $X_B$  of the junction point is empirically determined from data, i.e., the experimental exceedance probability curve  $P(X)_{B-I}$  and  $P(X)_{B-II}$  is used, and the combined exceedance probability analytical model is determined.

$$0 < X < \infty$$

$$P(X)_{B-I, II} \cong (1 - 1/4G_B) \cdot \delta(X) + \exp(-A) \cdot \sum_{m=0}^{\infty} (A^m/m!) \cdot (1/\sqrt{2\pi\hat{\sigma}_m^2}) \cdot \exp(-X^2/2\hat{\sigma}_m^2) \cdot (1/4G_B^2) \quad (6)$$

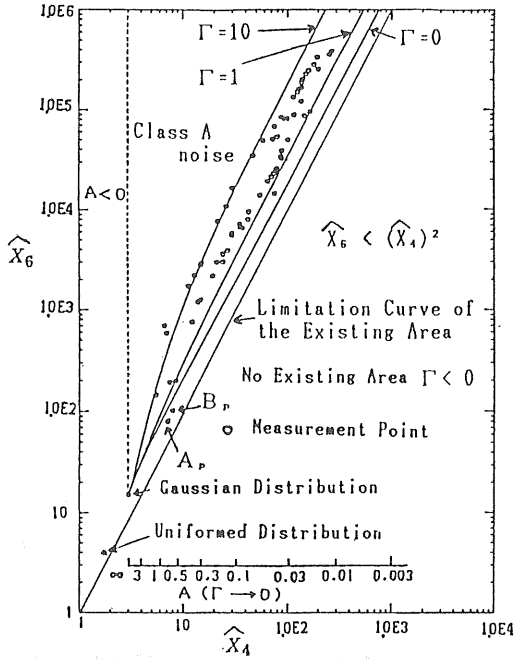


Fig. 7 Relation of  $\hat{X}_4$  and  $\hat{X}_6$ .

where,

$$\delta(X): \text{Delta function}$$

Figure 6 shows the schema of equation (1), (4), and (5) in which the applied parameters are  $\{A=0.015, \Gamma=5.0\}$  for Class A and  $\{A=0.045, \Gamma=7.0, A_r=1.0, \alpha=1.0, Ni=2.4, \text{ and } X_B=0.7\}$  for Class B. They are obtained by joining the two approximating forms  $P(X)_{B-I}$  and  $P(X)_{B-II}$  for the Class B interference model. As a results, the above Class B interference model is a similar with the Class A interference model.

At this point we will discuss interference voltage or current as the source of impulsive noise for electronic receiving circuits. If the impulsive noise is larger than  $X_B$ , we can apply the modified Class A interference model or the combined approximating forms  $P(X)_{B-I}$  and  $P(X)_{B-II}$  as the exceedance probability analytical model for Class B interference.

### 3. 4th and 6th-Order Moments

In Section 2-1, we discussed the parameters of the Class A interference. However, occasionally we obtained negative values can not be used to property formulate the exceedance probability as defined in the Class A interference model.

Normally, from equation (3a), (3b), and (3c) the normalized  $\hat{X}_1$  and  $\hat{X}_6$  by  $X_2$  are obtained.<sup>23</sup>

$$\hat{X}_4 = 3/A(1 + \Gamma)^2 + 3 \tag{7a}$$

$$\hat{X}_6 = 15/A^2(1 + \Gamma)^3 + 45/A(1 + \Gamma)^2 + 16 \tag{7b}$$

The equation (7b) is rewritten as shown.

$$\hat{X}_6 = 5(1 + \Gamma)(\hat{X}_4)^2/3 - 5(2\Gamma + 1)\hat{X}_4 + 15(\Gamma - 1) \tag{7c}$$

Gaussian random process with zero-mean or uniformed distribution are given as one parameter and dotted an independent point in  $(\hat{X}_4, \hat{X}_6)$  plane, however, the shaping parameters for impulsive noise are two and scattering in the  $(\hat{X}_4, \hat{X}_6)$  plane.

Equation (8) is plotted from measurement data at  $\Gamma=0, 1, \text{ and } 10$  (see Fig. 7) as the relation of normalized  $(\hat{X}_4, \hat{X}_6)$ . As results,  $(\hat{X}_4, \hat{X}_6)$  for Class A interference depends on shaping parameters  $(A, \Gamma)$ , and the existing area is  $\hat{X}_4 \geq 3, \Gamma \geq 0$ . If  $(\hat{X}_4, \hat{X}_6)$  are below the curve of  $\Gamma=0, \Gamma$  is negative values and not available for the Class A interference model. Point Ap and Bp are actually measured in the  $(\hat{X}_4, \hat{X}_6)$  plane, but these point are nearly Gaussian distribution, and thus are not impulsive noise. However, rectangular pulsvise Gaussian distribution is existing in the  $\Gamma < 0$  area and not existing in  $\hat{X}_6 < (\hat{X}_4)^2$  which is calculated theoretically:

$$\hat{X}_6/(\hat{X}_4)^2 \geq 1 \tag{9}$$

Thus, the Gaussian and uniformed distributions are shown by means of  $(\hat{X}_4=3, \hat{X}_6=15)$  and  $(\hat{X}_4=1.8, \hat{X}_6=3.86)$ .

### 3. Results

In base band communication, electrical signals are sent through communication links in the form of digital signals "1" and "0". This format is used in many types of digital information processing equipments such as computers or related equipments found in manufacturing, office, or laboratory areas.

Man-made impulsive noise, caused by machines or human bodies sometimes cause errors in digital circuits. If this impulsive noise is less than the threshold level of digital circuits, the information processing equipment will have no errors. However, the recent trend of information processing equipment are towards higher speed. Since noise threshold reduction is a necessary by-product in achieving higher speed, the possibility of error is increased. Before a discussion for errors in digital circuits, we consider errors caused of the noise sources for logic devices.<sup>23</sup> Lohstroh specified four category as the noise sources for logic devices,<sup>23</sup> and we applied Mid-

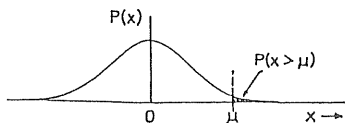


Fig. 8 Exceedance probability density function for  $X$ .

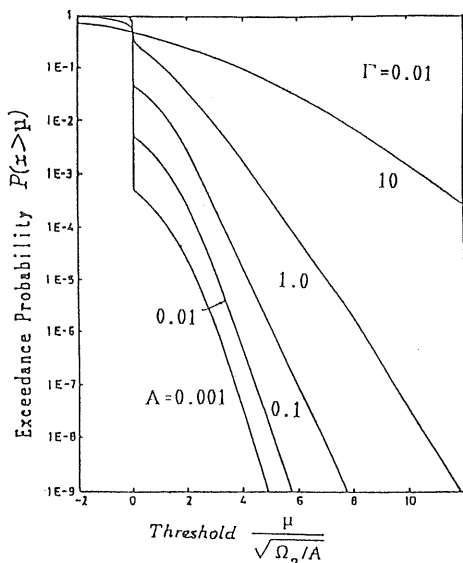


Fig. 9 Exceedance probability for threshold ( $\Gamma$ ).

Middleton's exceedance probability-density function to Lohstroh's noise source model of logic device in order to calculate bit error rates for digital circuits.

Figure 8 shows the exceedance probability-density function for  $X$ , where  $X$  is the amplitude of incoming signal of the digital circuits, and  $\mu$  is the threshold of the digital circuit input.

The error probability  $P(X > \mu)$  is given as shown below,<sup>6)</sup>

$$P(X > \mu) = \int_{\frac{\mu}{\sqrt{\Omega_2/A}}}^{\infty} \frac{1}{\sqrt{A(1+\Gamma)}} P(X) dx \quad (10)$$

Figure 9 shows the exceedance probability for threshold at  $\Gamma = 0.001$  as the parameter of  $A$ , where,  $\Gamma \ll 1$  with an existing small Gaussian background. Figure 10 is at  $A = 0.01$  as the parameter of  $\Gamma$ .

In base band communication, typical communication systems or digital circuits are required to achieve a very low error rate, less than the 9th power of 10 for impulsive noise between  $0.001 < A < 1$ , which corresponds to 5–12 times

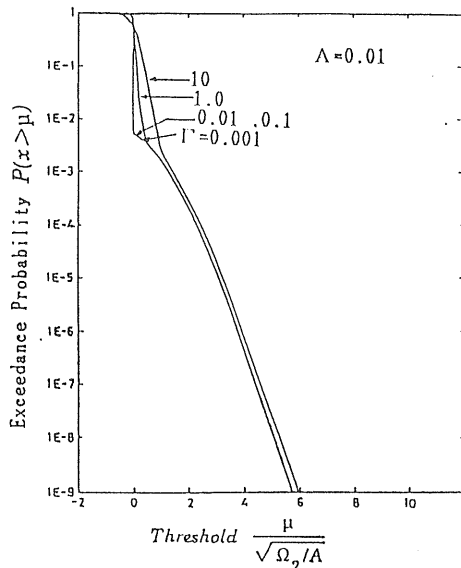


Fig. 10 Exceedance probability for threshold ( $A$ ).

for the threshold of peak interference impulsive noise.<sup>7)</sup>

#### 4. Conclusions

The purpose of this study has been to provide a method for determining the parameter of the approximate and exact analytical models of Class A and B interference. The above analytical model can be applied to urban electronic systems for calculating the bit error rates.

#### References

- 1) D. Middleton: IEEE Trans. Electromagn. Compat., EMC-19 (1977) 106
- 2) A. Sethapanee, N. Sudo, H. Higuchi, K. Yamauchi, M. Maeda, N. Morinaga and T. Nabe-kawa: IEICE Technical Report, EMCJ 87-88 (1988) 9
- 3) D. Middleton: IEEE Trans., Commun., COM-21 (1973) 1232
- 4) A. Spaulding: IEEE Trans., Commun., COM-33 (1985) 509
- 5) J. Lohstroh: IEEE J. Solid-State Circuits, SC-14 (1979) 591
- 6) K. Yamauchi, H. Higuchi, N. Takahashi and M. Maeda: IEICE Technical Report, EMCJ 88-40 (1988) 31
- 7) H. Higuchi, K. Yamauchi, N. Takahashi and M. Maeda: EMC International Symposium, Nagoya (1989) No. 1, pp. 209–213
- 8) K. Konishi and Y. Miyagaki: IEICE Technical Report, EMCJ 85-105 (1985) 19